American Journal of Modern Physics
2022; 11(2): 13-21
http://www.sciencepublishinggroup.com/j/ajmp
doi: 10.11648/j.ajmp.20221102.11
ISSN: 2326-8867 (Print); ISSN: 2326-8891 (Online)

Experimental Study on the Produce of Air Negative Ions from Liquid Water Evaporation

Peimin Pu[1, 2, 3, *], Jiangping Pu[1, 2], Zhengbin Zhu[1, 4]

[1]Cloud Water Engineering Inc. (CWEI), Nanjing, China

[2]Key Laboratory for Cloud, Fog Physical Environments, China Meteorological Administration in Chinese Academy of Meteorological Sciences, Beijing, China

[3]Nanjing Institute of Geography & Limnology, Chinese Academy of Sciences, Nanjing, China

[4]Faculty of Engineering, Computer and Mathematical Sciences, University of Adelaide, Adelaide, Australia

Email address:

jumpy@126.com (Peimin Pu), pupm2@qq.com (Jiangping Pu), robinzhu81@hotmail.com (Zhengbin Zhu)

[*]Corresponding author

To cite this article:

Peimin Pu, Jiangping Pu, Zhengbin Zhu. Experimental Study on the Produce of Air Negative Ions from Liquid Water Evaporation. *American Journal of Modern Physics*. Vol. 11, No. 2, 2022, pp. 13-21. doi: 10.11648/j.ajmp.20221102.11

Received: February 23, 2022; **Accepted**: March 21, 2022; **Published**: March 29, 2022

Abstract: It was revealed that liquid water surfaces, including water drop's surface might generate Negative Water Ions/molecules to air with probability of $(1/11)^8$ among the water surface molecules by the author's previous paper. Three experiments by spraying water from shower nozzle had been performed on a bathtub covered by soft plastic film with thickness of 10 mm during Aug.-Sep. 2019. The densities of negative ion (DNI) and the atmospheric parameters had been recorded. The experimental results showed that DNI increased immediately after spraying waters in orders with big variations. High DNI up to -190000 ion/cm^3 were recorded under spraying water temperatures about 45°C. The sliding averaged (for 10 instant values) DNI were direct proportion to differences of saturated vapor pressure of spraying water and air vapor pressure, and increasing of relative humidity (under constant air temperature). The liquid water drops become positively charged after evaporation with negative ions. After stopping water spray DNI might keep at high level in a short time interval, then decrease gradually with vibrations by processes of mixing and water phase exchange in a cloud-fog system with -/+ air ions. These experiments proved that neutral liquid water drops may generate air negative water ions/molecules by evaporation and positive charged water drops.

Keywords: Origin of Negative Ions in Atmosphere, Water Evaporation Generate Air Negative Ions, Ion Density Variation in Water Drops System, Water Drops Generate -/+ Ions, Safely Achieving High Negative Densities

1. Introduction

"What is the structure of water?" is the 46th one of the essential frontier 125 scientific issues [1]. A model for water (H_2O) molecule, the structure of ice, snow and liquid water were presented, and the reasons of formation of their specific characteristics were modeled in good coincidence with observed data [2, 3]. The liquid water surfaces, including drops, possess specific structure with porosity of 1:1 and are dominant by negative charges "-". We revealed that the liquid water surfaces might generate negative ions/ molecules (NWI, as the origin of negative ions in the atmosphere) to air with probability of $(1/11)^8$ among the water surface molecules by the author's previous paper. The NWI are occupied only $6/10^{15}$ of the evaporated water molecule [4]. There are mass/ energy exchange processes on the air-water boundary layer between water molecules at water skin surface and at around air under certain temperature and surface feature. Evaporation or condensation would be related with saturation state (or relative humidity) of water molecule close to water surface. When the water vapor pressure less than saturation one, the water molecules will leave from liquid water more than that condensed from air to liquid water surface. So the total electric charge of -5.7×10^5 C/s, and a mean current of 1800 electrons /cm^2/s, or total current of about 1500 A for the whole Earth surface [4, 5] might be released to atmosphere.

Therefore NWI provide the electrons from water/ground to air-atmosphere, similar the normal liquid water molecules provide the water volume to the atmosphere by evaporation. This is a balance of electricity in atmosphere, similar to the balance of water quantity: [evaporation and evaportranspiration (from ocean/ land) ↔ precipitation (from atmosphere and water content in atmospheric column)]. The mean volume of water in the atmospheric column with cross section of 1 cm^2 is 25.3 mm, which is equal to the volume of mean evaporation during 25.3/2.712=9.3 d. Similarly, mean number of electrons in the atmospheric column with cross section of 1 cm^2 is 7×10^5, which is the number of mean releasing electrons (negative water ion-molecules) from water surface during 6.48 min ($=7\times10^5$ /1800/60). Lightning transport "-" electricity to Earth surface, like rainfall transport waters to Earth surface. The stable state of net negative ions (electrons) in atmospheric column of 0-9 km is supported by water/ land surface, and the positive ions in the atmosphere, especially in the upper troposphere, is mainly supported by volcanic eruptions [4].

For verifying the fact that the negative ions are generated by evaporation from water surface, we arranged the experiments over a bathtub covered by soft plastic film with thickness of 10 mm to form a relatively closed space, using the shower nozzle for spraying water drops/ waterspout and cold/ warm water valves for controlling water quantity and temperature (Figure 1). Under the unsaturated condition the sprayed water drops would evaporate gaseous water molecules, some of them would be negatively ("-") charged- as negative ions. Meanwhile, part of the sprayed water drops, which evaporated "-" ions would be positively ("+") charged. This process may generate both "-" and "+" ions. After long time spraying water, especially warm water (the maximum temperatures were controlled by 47-51°C). The air masses and heat would be mixed by turbulences and radiation (including the spraying nozzle after spraying warm water has thermal capacity and decreasing temperature by infrared radiation and turbulence thermal exchange with environments), associated with water evaporation/ condensation and "-/+ ion" generation/ dissipation like in cloud/ fog system. The ion-monitoring instrument attracts air into its sensor and might record the density of ion in air around the mouth of the instrument. It would record the time-space inhomogeneous distributed density of air ions. The experimental results were summarized in this paper.

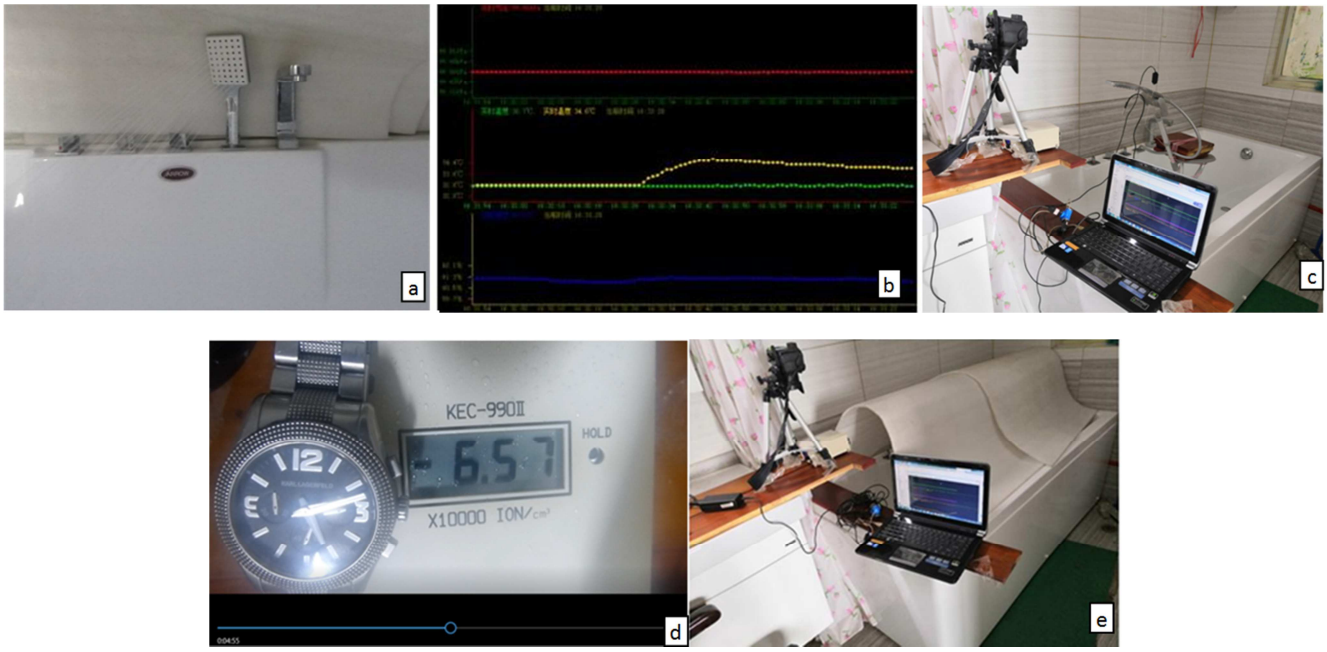

Figure 1. *Instrumentation: a) Shower nozzle and bathtub of Arrow brand were used; the nozzle has surface area of 9×11 cm^2, with 6×8 holes of diameter 1 mm, total output of about 2g/s/hole (water release intensity is about rainstorm on 1m^2 ground); b) The air temperature, relative humidity, atmospheric pressure and water temperature had been recorded in computer by using SHT75 sensors made in Switzerland by SENSIRON Ltd; assembled by Nanjing U. of Information Engineering; c) The air parameter sensors are settled over the shower nozzle (near the top cover) and the water temperature sensor is under the shower nozzle in the waterspout; all the data are recorded in computer. The instrument of KEC-900 II / 990II made in Japan was used for numerical monitoring the "-/+" ion densities by absorb air in front of it and the data were recorded by video recorder (LICA-V-LUX 3, made in Japan) and watch, as shown in d); e) The bathtub was covered by soft plastic film of 1 cm thickness during the experiments).*

2. Instrumentation and Experiments Overview

The experiments were performed over a bathtub with soft plastic cover with thickness of 1 cm (Figure 1). The shower nozzle and bathtub of Arrow brand (170×85×60 cm) were used; the nozzle has surface area of 9×11 cm^2, with 6×8=24 holes of diameter 1 mm, total output of about 2g/s/hole (water release intensity is about rainstorm on 1m^2 ground) (Figure 1.a). The air temperature, relative humidity, atmospheric pressure and water

temperature had been recorded in computer by using SHT75 sensors made in Switzerland by SENSIRON Ltd; assembled by Nanjing U. of Information Engineering; (Figure 1.b). The air parameter sensors are settled over the shower nozzle (near the top cover) and the water temperature sensor is under the shower nozzle in the waterspout; all the data are recorded in computer. (Figure 1.c); The instrument of KEC-900 II / 990II made in Japan (with digital display) was used for numerical monitoring the "-/+" ion densities by absorb air in front of it and the data were recorded by video recorder (LICA-V-LUX 3, made in Japan) and watch, as shown in (Figure 1. c, d); The bathtub was covered by soft plastic film of 10 mm thickness during the experiments (Figure 1.e).

3. Results

3.1. Test I: Started from 28 Aug. 2019 at 10h 40' 20" (Total 535s, the Mean Atmospheric Pressure Was 100.6 hPa)

After collecting the background information the cold water spraying valve was opened at No. 105 (according to the negative ion display number, back ground information was No. 0-104, Figure 2.a). The warm water valve was opened at No. 228. The cold water valve was closed at No. 240. The warm water valve was closed at No. 455. The water temperature in pipe was different with air temperature and inhomogeneous. Therefore the spraying water temperature had complex pattern (Figure 2.b).

The evaporation rate (E) from plane water surface is in direct proportion to the difference of saturated water vapor pressure at water surface temperature e_s and vapor pressure close to the water surface $e_a=(e_{sa}f)$, f-relative humidity [5-9].

$$E = \alpha\Delta e\,,\ (e_s - e_a)\,,\ e_a = e_{sa}f\,; \tag{1}$$

Where may use empirical formula as:

$$e_s(t) = 6.112\times \mathrm{EXP}((17.67\times t)/(t+243.5)) \tag{2}$$

$$\alpha = (22.0 + 2.0(t_s - t_a) + 12.5W_{1.5}^{2})^{1/2}\,; \tag{3}$$

Where t_s-water surface temperature, t_a- air temperature. $W_{1.5}$-wind speed at elevation 1.5 m above ground, here might be assume as spraying water speed.

Except above main elements, processes of evaporation-condensation from water drops related with radius, static electricity and dissolved substances possess more complex characteristics [10]. For qualitatively reveal the produce of air negative ions by water evaporation we may use the simplified models. In case when we spraying warm water we have large t_s-t_a; when the t_a≈const, increasing f means increasing evaporation rate.

The back ground was: in bathtub with water and soft plastic cover of thickness of 1 cm; there were fluctuations with mean negative ion density of -1576 ion/cm^3 (Figure 2.c). The water temperature t_s, air temperature t_a, and relative humidity f kept stable and the relative humidity decreased slightly after the bathtub enclosed by soft plastic cover, which might be influenced by mixing of air mass after covering soft plastic cover (Figure 2.b).

After spraying cooled water the water temperature increased (it means the water in the tube had more temperature then that of water sensor and air temperature over bathtub), the relative humidity and density of negative ions being increased. It indicated that the process of increasing negative ions is generated by evaporation process. The mean density of negative ions increased from -1577±430 ion/cm^3 into -6808 ion/cm^3 and the maximum value was recorded as -19700 ion/cm^3 during 75s (Figure 2.c,d). Meanwhile, the water temperature increased from 28.8 to 29.8°C, and the relative humidity increased from 88.4 to 91.6%, the air temperature kept almost stable, as showed in Figure 2.b.

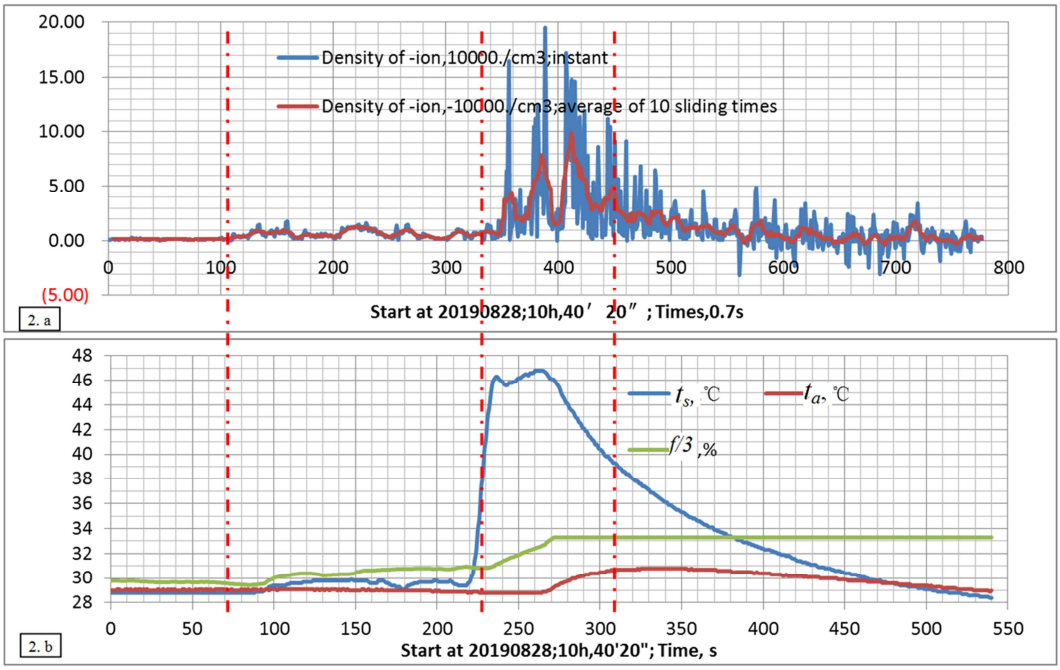

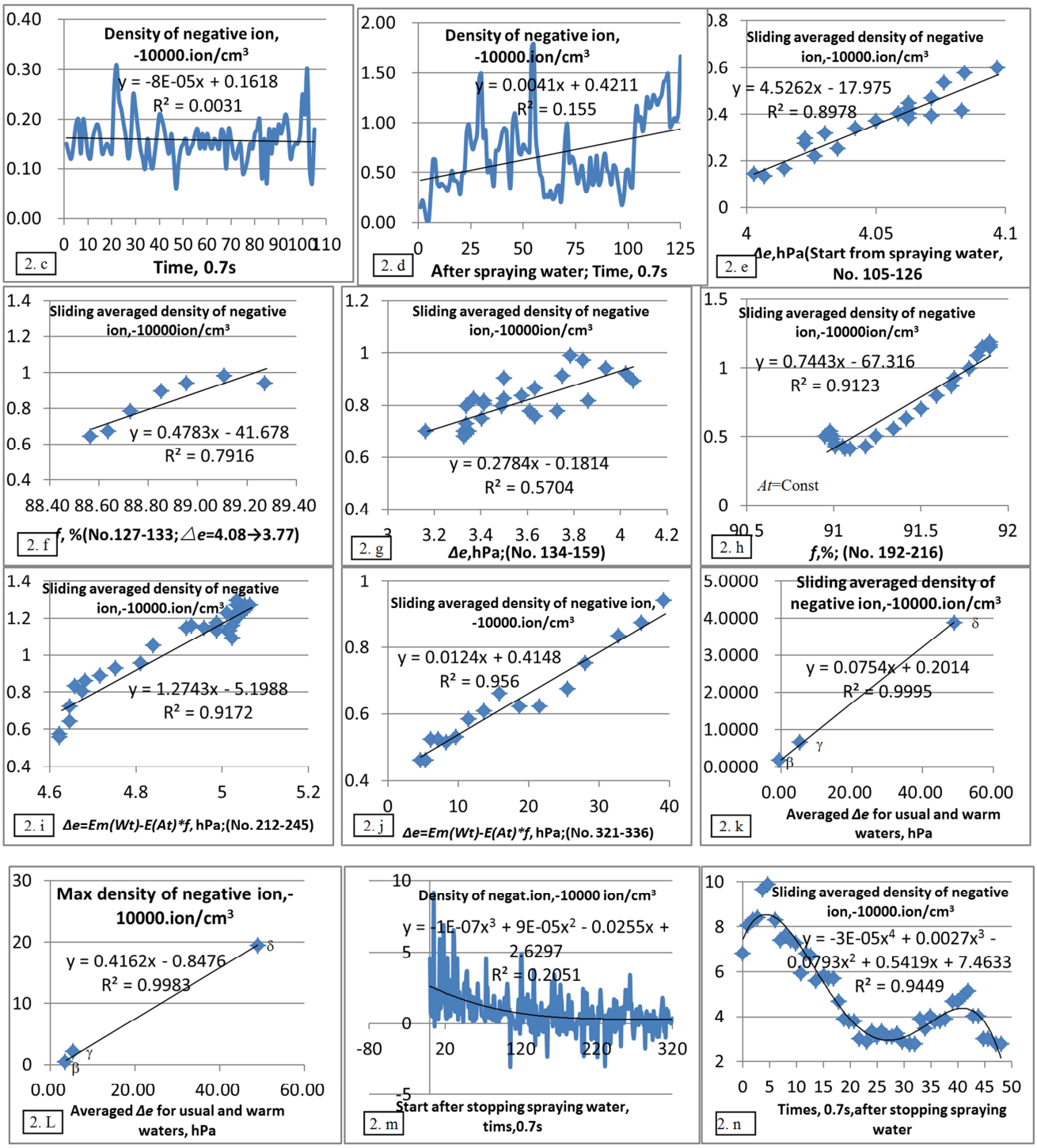

Figure 2. *Test I: Started from 28 Aug. 2019 at 10h 40' 20" (Total 535s, the Mean Atmospheric Presure was 100.6 hPa). 2. a), Variation of Density of –ion, 10000/cm³; ----instant and ----average of 10 sliding times in relation with 0.7s; 2. b), Variation of water temperature ts°C, air temperature ta°C, and relative humidity f/3, % in relation with time s; 2. c), Started from 28 Aug. 2019 at 10h 40'20". Variation of Density of negative ion, -10000.ion/cm³, in relation with 0.7s; 2. d), Variation of Density of negative ion, -10000.ion/cm³, in relation with time 0.7s after spraying tap water; 2. e), Relatioship between Sliding averaged density of negative ion,-10000.ion/cm³ and Δe, hPa, Started from spraying water, No. 105-126 (in Figure 2.a); 2. f), Relationship between Sliding averaged density of negative ion,-10000ion/cm³ and f, % (No. 127-133 [in Figure 2.a]; Δe=4.08→3.77); 2. g), Relatioship between Sliding averaged density of negative ion,-10000.ion/cm³ and Δe, hPa, Started from spraying water, No. 134-159 (in Figure 2.a); 2. h), Relatioship between Sliding averaged density of negative ion,-10000.ion/cm³ and Δe, hPa, Started from spraying water, No. 192-216 (in Figure 2.a); 2. i), Relatioship between Sliding averaged density of negative ion,-10000.ion/cm³ and Δe=Em(Wt)-E(At)*f,hPa, No. 212-245 (in Figure 2.a); 2. j), Relatioship between Sliding averaged density of negative ion,-10000.ion/cm³ and Δe=Em(Wt)-E(At)*f,hPa, No. 321-336 (Figure 2.a); 2. k), Relatioship between Sliding averaged density of negative ion,-10000.ion/cm³ and averagedΔe for before spraing ( ), spraying usual tap water ( ) and warm waters ( ), hPa; 2. l), Relatioship between Maximum density of negative ion,-10000.ion/cm³ and averagedΔe for before spraing ( ), spraying usual tap water ( ) and warm waters ( ), hPa; 2. m), Variation of Density of negative ion, -10000.ion/cm³, in relation with time 0.7s after stopping spraying waters; 2. n). Variation of Sliding Density of negative ion, -10000.ion/cm³, in relation with time 0.7s after stopping spraying waters.*

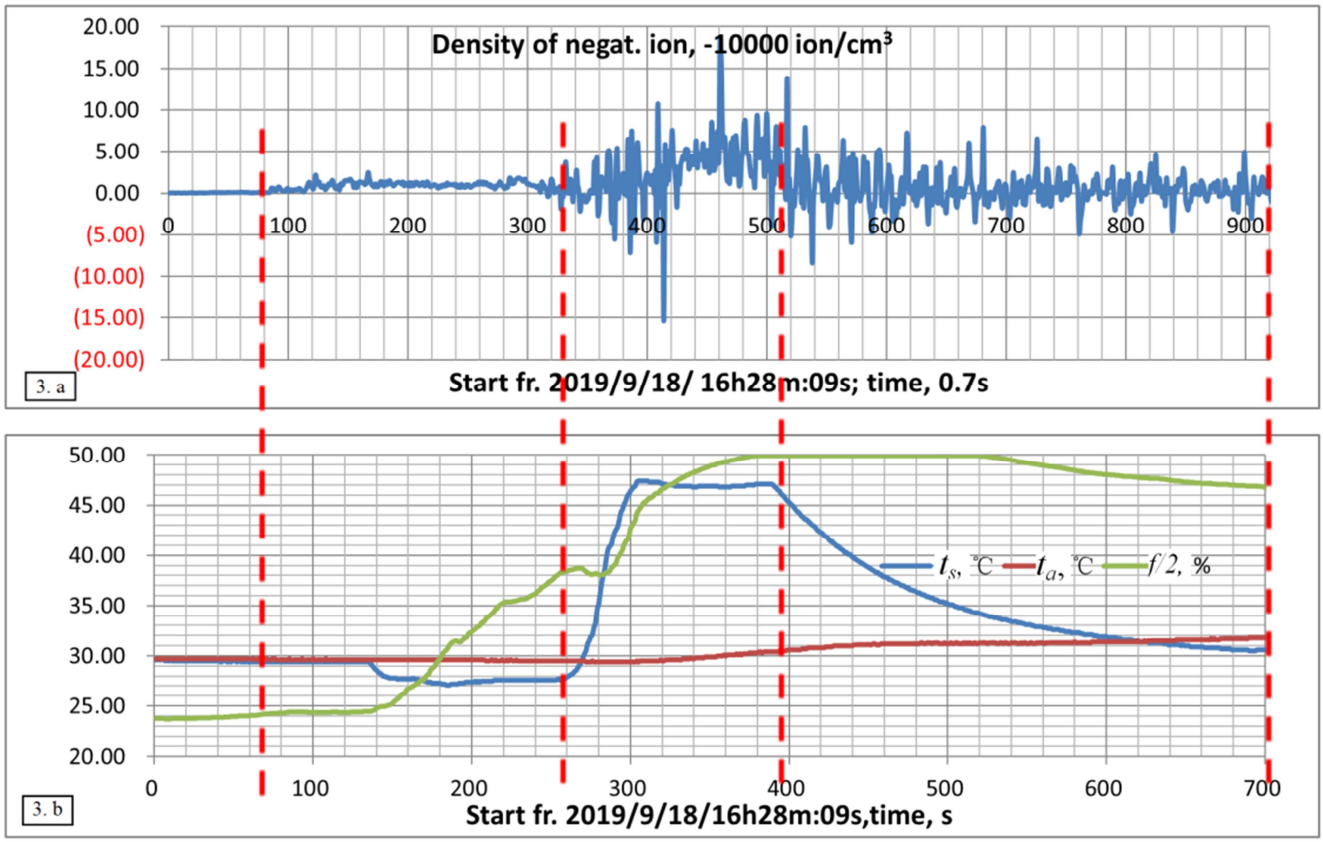

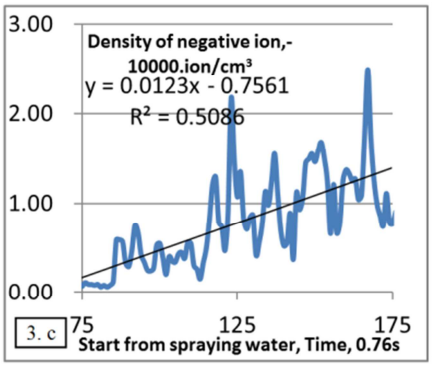

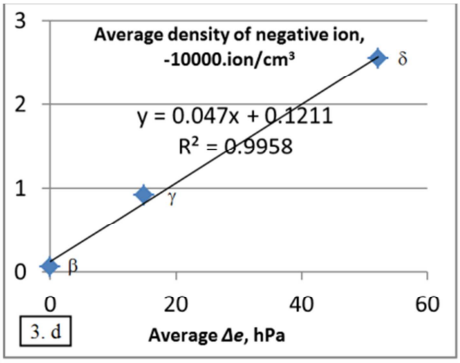

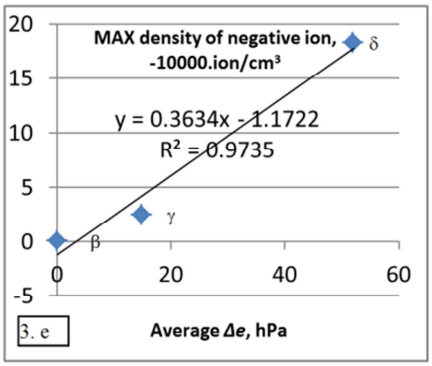

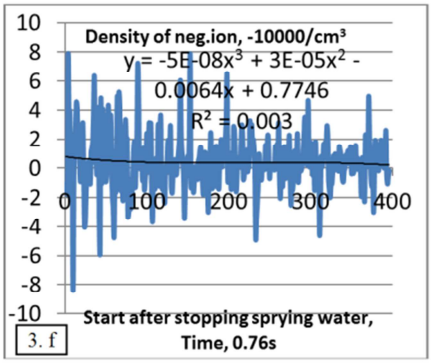

Figure 3. *Test II: Started from 18 Sept. 2019 at 16h 28'09"; The Mean Atmospheric Pressure Was 101.52 hPa.3. a), Variation of Density of –ion, 10000/cm³ in relation with time 0.7s; 3.b), Variation of water temperature t_s°C, air temperature t_a°C, and relative humidity f/2, % in relation with time s; 3. c), Variation of Density of negative ion, -10000.ion/cm³, in relation with time 0.76s start from spraying tap water; 3. d), Relatioship between averaged density of negative ion,-10000.ion/cm³ and averagedΔe,hPa, for before spraying ( ), spraying usual tap water ( ) and warm waters ( ); 3. e), Relatioship between Maximum density of negative ion,-10000.ion/cm³ and averagedΔe, hPa, for before spraing ( ), spraying usual tap water ( ) and warm waters ( ); 3. f). Variation of Density of negative ion, -10000.ion/cm³, in relation with time 0.76s after stopping spraying waters.*

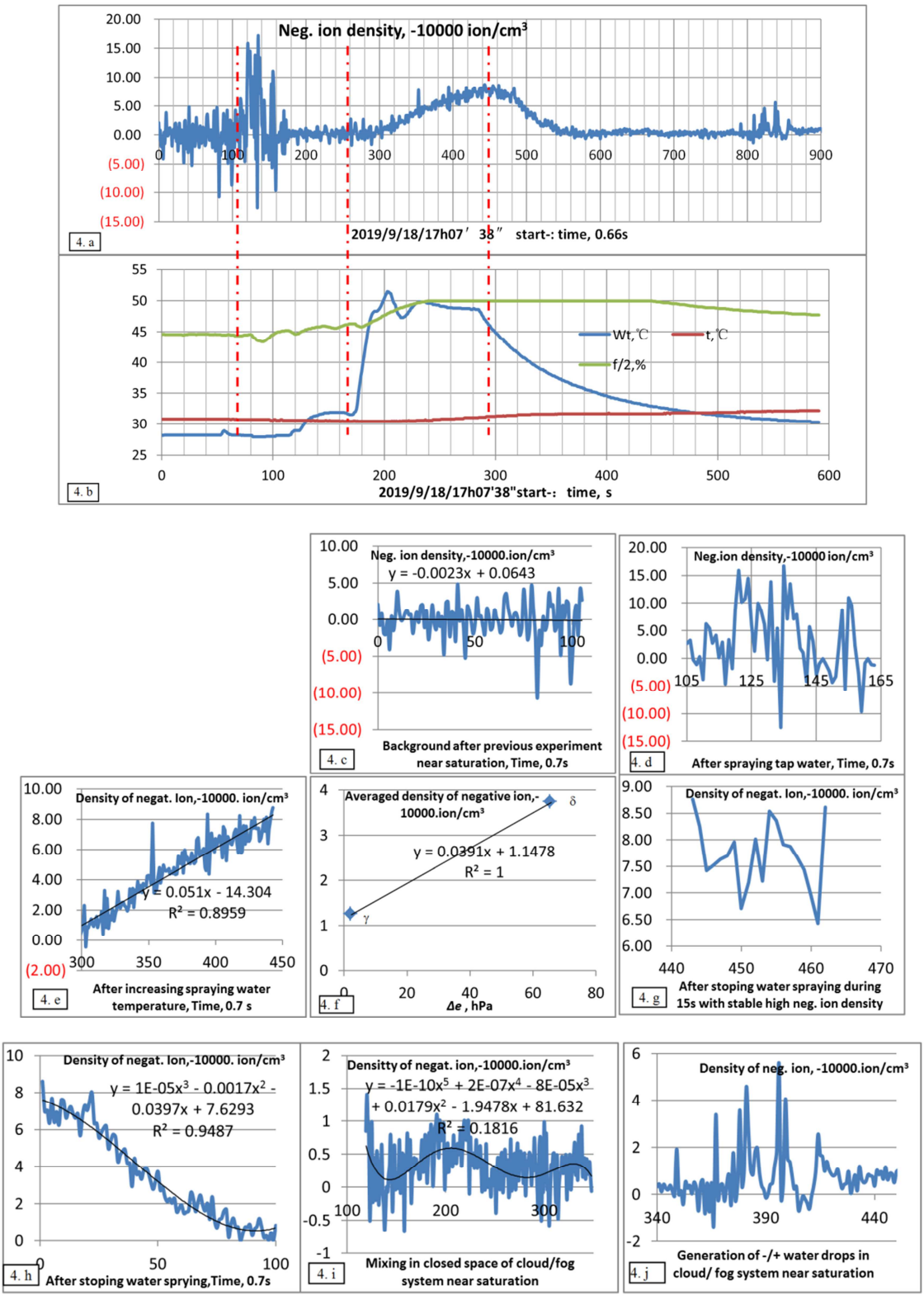

Figure 4. *Test III. Started from 18 Sept. 2019 at 17h 07'38"; The Mean Atmospheric Pressure Was 101.54 hPa. 4. a), Variation of Density of negative ion, -10000/cm³ in relation with time 0.66s; 4. b), Variation of water temperature Wt°C, air temperature t°C, and relative humidity f/2, % in relation with time s; 4. c), Variation of Density of negative ion, -10000.ion/cm³, in relation with time 0.7s, as background after previous experiment near saturation; 4. d), Variation of Density of negative ion, -10000ion/cm³ after spraying tap water in relation with time 0.7s; 4. e), Variation of Density of negative ion, -10000ion/cm³ after increasing spraying water temperature in relation with time 0.7s; 4. f), Relatioship between averaged density of negative ion,-10000.ion/cm³ and averagedΔe,hPa, for spraying usual tap water ( ) and warm waters ( ); 4. g), Variation of Density of negative ion, -10000ion/cm³ after stopping water spraying during 15s with stable high negative ion density; 4. h), Variation of Density of negative ion, -10000ion/cm³ after stopping water spraying with time, 0.7s; 4. i), Variation of Density of negative ion, -10000ion/cm³ with time 0.7s in closed space under cloud/ fog system near saturation; 4. j). Generation of -/+ water drops in cloud/ fog system near saturation with large pulse series of -/+ ion densities, -10000.ion/cm³.*

Sliding averaged DNI has more stable characteristics. It was found that the sliding averaged (for 10 instant values) DNI increased with evaporation rate (Eq. 1: $E \propto \Delta e$) (Figure 2.e) during No. 105-126 in Figure 2.a. These two parameters (E, and Δe) were in direct correlation with high correlation coefficient; also as showed in Figures 2.g, i, j. In case of intensive convection the generated negative ions might upward together with air mass to increase the relative humidity ($t_a \approx$Const.) as showed in Figure 2.f, h. If we average the data in lager time interval, we may find more common regular pattern as shown in Figure 2.k, [Sliding averaged (for 10 instant values) DNI increased with averaged Δe during before (β) (No. 0-110), after spraying usual (γ) (No. 110-340) and warm (δ) (No. 340-460) waters]. Relationship of maximum DNI with averaged Δe during before (β) (No. 0-110), after spraying usual (γ) (No. 110-340) and warm (δ) (No. 340-460) waters with maximum of -194900 ion/cm^3 was shown in Figure 2.L. All these indicated that the spraying water generated negative ions by liquid water evaporation.

After stop of spraying water, the DNI would have decreasing tendency with pulses by coagulation, merger, collision, and formation/ reformation of liquid drops with different scales. For example, under similar temperature, humidity and air pressure conditions, the smaller water drops easier be evaporated and bigger drops easier be condensed absorb gaseous state water. The water drops lost "-"ions by evaporation and become "+" liquid water ions. Therefore, the big pulse of +/- ion density might be monitored, such as -91500.ion/cm^3, -34000.ion/ cm^3, and +30500.ion/ cm^3 (Figure 2.m). The processes would be similar what are in cloud/ fog systems. Sliding averaged DNI may decrease fluctuations of small scales and reveal variation with larger scales (Figure 2.n). The processes of production and dissipation of ions are coexisted in nature. The distribution of density of -/+ ion in time/ space may have very complex characteristics.

3.2. Test II: Started from 18 Sept. 2019 at 16h 28' 09"; The Mean Atmospheric Pressure Was 101.52 hPa

Before spraying water, the averaged DNI was -743 ion/cm^3, after spraying water the density of negative ion increased to the maximum of -24900. ion/ cm^3, during 75-175s as shown in Figure 3.a, c. Sliding averaged (for 10 instant values) DNI increased with averaged Δe during before (β) (No. 0-75 in Figure 3.a), after spraying usual (δ) (No. 75-325 in Figure 3.a) and warm (γ) (No. 325-528 in Figure 3.a) waters (Figure 3.d). Maximums DNI were related with averaged Δe during before (β) (No. 0-75 in Figure 3.a), after spraying usual (γ) (No. 75-325 in Figure 3.a) and warm (δ) (No. 325-528 in Figure 3.a) waters (Figure 3.e). Variations of DNI, after stopping spraying waters were shown in Figure 3. f.

All above information indicates that the negative ions are generated by evaporation of liquid water. Water drops evaporate vapor molecules, including negative ions become positive ion-water drops. Condensation may generate negative water drops by negative ions. Therefore, there are both the -/+ ions in the system. After stopping spraying water the cloud/fog system may has decreasing tendency of the averaged DNI, but with -/+ picks of ion density of -78600.ion / cm^3 and +84000.ion/ cm^3 (Figure 3.f).

3.3. Test III. Started from 18 Sept. 2019 at 17h 07'38"; The Mean Atmospheric Pressure Was 101.54 hPa

This experiment was performed after previous one with warm water (45.5°C) spraying. The previous experiment was stopped at 27′ before and under soft plastic cover. The conditions at the beginning of this experiment were $f \approx$98.4%, air temperature $t_a \approx$30.8°C, water spraying nozzles temperature $t_s \approx$28.2°C$<t_a$. The condensation would be happened round the metallic nozzles with vertical/ horizontal mass mixing processes. This stage was similar what in weakening cloud/fog system with low averaged negative ion density and fluctuations of -/+ ion density (Figure 4.a, b, c). After spraying tap water, the negative ion density increased with mean value of -41712.ion/cm^3, maximum peaks of -166700.ion/cm^3 and +125200.ion/cm^3 (Figure 4.d). After spraying warm water, when the water temperature was much higher than air temperature, the evaporation were increased steady and very intensively and observed steady increasing of DNI with maximum of -87600 ion/cm^3 (Figure 4.e). The evaporation rate is direct proportional to Δe (Eq. 1, 2). The sliding averaged (for 10 instant values) DNI after spraying usual water (β) and warm water (δ) close related with Δe (Figure 4.f). It means the air negative ions are generated by evaporation of water. After stopping water spraying a high DNI mean value of -70792.ion/ cm^3 was observed during 15s (Figure 4g); but it could not keep for long time and gradually decreased with different frequency scales of vibrates (Figure 4.h-j).

4. Conclusion

4.1. Negative Air Ions Were Generated by Evaporation from Liquid Water Surface as Negative Water Ions (NWI)

As well now, there are "-/+" (negative/ positive) ions in troposphere. Where are they come from? We revealed that the liquid water surfaces might generate negative ions/ molecules (NWI, as the origin of negative ions in the atmosphere) to air with probability of $(1/11)^8$ among the water surface molecules by the author's previous paper [4]. Therefore, the more evaporation rate is the negative ion density will be more. Here the generation and variation processes of NWI might be described in detail by above three experiments.

For example, the Test I showed: the averaged density of negative ion (DNI) from -1577±430 ion/cm^3 (as background of experiment I in Figure 2.c) increased into -6808 ion /cm^3 and the maximum value was recorded as -19700 ion/cm^3 during 75s (Figure 2.d). The sliding averaged (for 10 instant values) DNI increased with increasing of evaporation rate in direct correlation (Figure 2.e, g, i, j), with increasing of humidity under $t_a \approx$Const. (which should be supported by evaporation from liquid water, Figure 2.f, h). The relationship

of sliding averaged (for 10 instant values) DNI increased with averaged Δe (Eq. 1, 2) during before (-1577./cm^3, β), after spraying usual (-6460./cm^3, γ) and warm waters (-38809.ion/cm^3, δ) (Figure 2.k); the maximum DNI may reach -194900.ion/cm^3 (δ) for spraying warm water and -17900.ion/cm^3 (γ) for spraying usual tap water (Figure 2.L).

The similar results were showed by the Test II:

Before spraying water, the averaged DNI was -743 ion/cm^3, after spraying water the DNI increased to the maximum of -24900. ion/ cm^3, during 75.0s as shown in Figure 3.a, c. The relationship of sliding averaged (for 10 instant values) DNI increased with averaged Δe (Eq. 1, 2) during before (-560.ion/cm^3, β), after spraying usual (-9189./cm^3, γ) and warm waters (-25417.ion/cm^3, δ) (Figure 3d); the maximum density of negative ion may reach -182800.ion/cm^3 (δ) for spraying warm water and -24900.ion/cm^3 (γ) for spraying usual tap water (Figure 3.e).

Main results of the Test III:

This experiment was performed after previous one with warm water (45.5°C) spraying. The previous experiment was stopped at 27 min before and under soft plastic cover. The conditions at the beginning of this experiment were f≈89.2%, air temperature t_a≈30.8°C, water spraying nozzles temperature t_s≈28.2°C< t_a. The condensation would be happened on the metallic nozzle (t_s< t_a) with vertical/ horizontal mass mixing processes. This stage was started similar what was in cloud/fog system with averaged +552 ion/cm^3 (close to ion-free state), but maximum peaks of -48300 ion/cm^3 and +107400 ion/cm^3 (Figure 4.c); which indicates that there are many liquid water particles with +/- ions. The negative ion density after spraying tap water was rapidly increased to mean value of -41712ion/cm^3, with maximum peaks of -166700 ion/cm^3 and +125200 ion/ cm^3 (Figure 4.d). When the water spraying water temperature was much higher than air temperature, the evaporation were increased steady and very intensively with time and the DNI was recorded the maximum value of -87600 ion/cm^3 (Figure 4.e). The sliding averaged (for 10 instant values) DNI increased with averaged Δe after spraying usual (γ) (No. 105- 258, in Figure 4.a) and warm (δ) (No. 258-445, in Figure 4.a) waters (Figure 4.f). All these indicated that the air negative ions were generated by evaporation of sprayed waters (liquid water evaporation).

4.2. After Stopping Spraying Water in the "cloud/fog" System Close to the Saturation Conditions May Generate Picks of "-/+" Ion Densities

After stopping spraying (warm) water in the "cloud/fog" system close to the saturation conditions may keep high density of negative ion for a time, for example: 1) with sliding peak of -98710 ion/cm^3 in Test I (Figure 2.m); 2) -78600/ +84000 ion/cm^3 in Test II (Figure 3.f); 3) stable high negative ion density during 15 s with averaged negative ion of –77100 ion/cm^3 in test III (Figure 4.g). In such cloud/fog systems should exist condensation/evaporation processes to form liquid water droplets, starting from minimum scale droplets, then form droplets with bigger and bigger scales; then form "-/+" peaks of ion density. (Figure 2.m, n. Figure 3.f. Figure 4.c, g-j). The averaged density of -/+ions were decreased with time in general.

4.3. The Observed Natural Data Accord with the Experiments Results, the New Technology for Generating Negative Air Ions Might Be Developed

The observed natural data show that the densities of negative ions are rich in areas near falls [10], in caves with water drops, ponds and small streams [11], forests [12-17], close to sea cost [18, 19]. The air negative ions are benefit to human health [20, 21], and the artificial generated air negative ions by usual techniques may associate with generation of ozone, which may be hazardous to human health [22], so the new technology for generating negative air ions might be developed on the basis of above experiments, even possible to develop instrument for treatment disease, such as COVID-19. The space- time characteristics of negative ions observed in nature may be explained by production theory of the negative ions by evaporation/ evapotranspiration from the water/ land/ plants and evolution dynamics of the -/+ ions by heat conductivity (turbulence, convection, collision and radiation) and liquid ↔ gaseous phase transformation as described in above section 3.

5. Recommendations

5.1. Increasing Visibility Along Highways by Using Stainless Steel Net Supported by Safety DC +/- 24 V

The experiments showed that there are much high concentrations of -/+ ions in "cloud/ fog system". The aerosols near ground also possess electric charges. Therefore, we may use stainless net supported by safety DC +/- 24 V along highways to absorb water droplets and aerosols to increase the visibility in cases of fog and haze. The system may be intelligently controlled.

5.2. Searching New Technologies for Production of "Negative Ions Generator"

We may develop technologies to generate high negative ion density for daily use and medical treatments without release any toxic elements based on the research results of this article.

5.3. Searching New Approaches for Weather Modification

We may use the waste heat released by airplane to increase the spraying water droplets to generate gigantic gaseous/ liquid/ solid state waters with different +/-/neutral charged particles, to rapid change the dynamic movement and the structure in cloud and to find possible approaches for quickly growth of lager snow/ice/graupel, then to form water precipitation. A series of experiments need to be studied.

Supplementary Information

This article is supported by Key Laboratory for Cloud / Fog

Physical Environments, China Meteorological Administration in Chinese Academy of Meteorological Sciences; Beijing China under subject of "Research and experiment on capacity building of weather modification in the northwest region" with Contract: ZQC-R18169/RYSY201904.

Authors Contributions

The authors had discussed the experiments approaches.

Acknowledgements

We are grateful for the supporting of the instrument of KEC-900II/990II by Research Prof. Shiliang Fan (Nanjing Tembusu Advanced Materials Institute, Nanjing, China) and the recording system of atmospheric air pressure-temperature-relative humidity –water temperature by Eng. Hanfeng HU of Nanjing Information Engineering University (Nanjing, China).

References

[1] Kennedy, D., Norman, Cc. (2005). *Science*, 125th Anniversary, Special Issue 309, pp. 75.

[2] PU, P. M. PU, J. P. ZHU, Z. B. (2016). Study on the structure model of water molecule and the reasons of formation of some characteristics of liquid & solid water. *J. of Meteorological Sciences*, 36 (5): 567-580 (in Chinese).

[3] PU, P. M., PU, J. P., ZHU, Z. B. (2020). Study on the Structure Model of Water Molecule and the Reasons of Formation of Some Characteristics of Liquid & Solid Water. *American J. of Modern Physics*, (2): 11-27. ISSN: 2326-8867 (Print); ISSN: 2326-8891 (Online). SciencePG.

[4] PU, P. M., PU, J. P., ZHU, Z. B. (2017). Liquid water skin structure & its influence on atmospheric electric fields; *SCIREA J. of Geosciences*, 2 (2): 39-55. (http://www.scirea.org/journal/PaperInformation?JournalID=17000&PaperID=334) (http://article.scirea.org/pdf/17010.pdf;)

[5] PU, P. M. (1994). Studies on the formulae for calculating evaporation and heat loss coefficient from water surface in China (I), *J. of Lake Sciences*, 6 (1): 1-12 (in Chinese).

[6] PU, P. M. (1994). Studies on the formulae for calculating evaporation and heat loss coefficient from water surface in China (II), *J. of Lake Sciences*, 6 (3): 201-210 (in Chinese).

[7] CHEN, H. Q., MAO, S. M. (1995). Calculation and verification of an universal water surface evaporation coefficient formula, Advances in water science, 6 (2): 116-120 (in Chinese).

[8] MAO, R., GAO, J. F., (1996). Water evaporation from various water surface, *Oceanologia et Limnologia Sinica*, 27 (4): 445-450 (in Chinese).

[9] WANG, J. Q. (1990). *Some experimental study on evaporation in Northern China*, Science Press, Beijing, China, 48-53 (in Chinese).

[10] P. N. Tverskoi. Ed. (1951). Course of meteorology. (Hydromet Press, Leningrad, USSR). (in Russian); 413-471-495.

[11] YU, J., GAO, Z. D, *et al.*, (2021). Analysis of temporal and spatial distribution characteristics and influencing factors of air anions in Tianyuan cave, *Environmental Chemistry*, 40 (4): 1078-1087 (in Chinese).

[12] SHAO, H. R., HE, QT., Forest and Air Anion, *World Forestry Research*, 13 (5): 19-23 (in Chinese, 2000).

[13] BING, L. F., LI, X. Z., *et al.* (2009). An experimental formula about the evapotranspiration of reference vegetation on northern slope of Great Hing'an Mountains, *Chinese J. of Ecology*, 28 (1): 67-171 (in Chinese).

[14] XU, M., CHEN, B. F. g, *et al*. (2008). Dynamic of negative air ions and its relationship to environmental factors in Maofeng Mountain, Guangzhou, *Ecology and Environment*, 17 (5): 1891-1897 (in Chinese).

[15] WANG. W., (2014). Characteristics of negative air ion concentration and its relationship with environmental factors, *Ecology and Environmental Sciences*, 23 (6): 979-984 (in Chinese).

[16] Meng, J. J., ZHANG, Y., (2000). Electrical discharge of plant pointed ends-main source of air ions on ground, *Environmental Science and Technology*, 28 (1): 788-792 (in Chinese).

[17] SI. T. T., LUO. Y. J., *et al*. (2015). Negative Air Ion Concentration Under Fog Conditions in Diaoluoshan Tropical Rainforest and Their Relations with Selected Meteorological Elements, *J. of Hainan Normal University (Natural Science)*, 28 (2): 199-202 (in Chinese).

[18] Vana, M., Ehn, M., *et al*; (2008). Characteristic features of air ions at Mace Head on the west coast of Ireland, *Atmospheric Research*, 90 (2): 278-286.

[19] LI. X. Z., WANG, J. Q., (1992). Seashore climate and air negative ions, *Navy Medicine*, 10 (1): 67-69 (in Chinese).

[20] LIN Zhongning, The effects of air negative ion on health care, Ecologic Science, 18 (2): 87-90 (in Chinese, 1999).

[21] Badhe Ravindra V.; Nipate Sonali S. (2021). The use of negative oxygen ion clusters [$O_2^-(H_2O)n$] and bicarbonate ions [HCO_3^-] as the supportive treatment of COVID-19 infections: A possibility, *Journal of Medical Hypotheses*, 154.

[22] CAO, H., HOU, W. P., *et al*. (2015). Design of low ozone anion haze air purifier, *Forest Engineering*, 231 (2): 119-121.